# 12

Karp, Tobias, Christopher A. Scholz, and Michael M. McGlue, 2012, Structure and stratigraphy of the Lake Albert Rift, East Africa: Observations from seismic reflection and gravity data, *in* O. W. Baganz, Y. Bartov, K. Bohacs, and D. Nummedal, eds., Lacustrine sandstone reservoirs and hydrocarbon systems: AAPG Memoir 95, p. 299–318.

# Structure and Stratigraphy of the Lake Albert Rift, East Africa: Observations from Seismic Reflection and Gravity Data

**Tobias Karp[1], Christopher A. Scholz, and Michael M. McGlue[2]**

*Department of Earth Sciences, Syracuse University, Syracuse, New York, U.S.A.*

## ABSTRACT

Modern lake basins set within active continental rifts provide useful analogs for exploration efforts in ancient extensional basins that are known to be rich in hydrocarbons. Lake Albert is one of the Great Lakes of Africa and is located at the northern end of the western branch of the East African rift system. This large, but comparatively shallow, eutrophic, and probably geologically ephemeral lake basin serves as an end-member example of the modern tropical lake systems that occupy this extensional province. Seismic reflection and gravity data sets indicate that the basin contains a maximum of 5 km (3.1 mi) of synrift, dominantly lacustrine sedimentary fill, in two subbasins separated by a midbasin high. In contrast to other large rift basins in the western branch of the rift valley, the Lake Albert Rift is not a highly asymmetrical half-graben basin, but instead has subsided nearly symmetrically and continuously in the late Cenozoic along two extensive boundary fault systems on either side of the basin. Seismic sequences from across the basin were correlated to borehole stratigraphy from a deep well drilled on the Ugandan margin. These observations suggest that the basin has experienced a long-term change from a continuously open lacustrine, possibly deep lake system in the Miocene or early Pliocene, to an alternating shallow lacustrine and fluvial system in the mid and late Pleistocene. This history of basin evolution has led to the development of a rich hydrocarbon system.

## INTRODUCTION

Organic-rich rocks of lacustrine origin are the dominant source of hydrocarbons in many oil and gas provinces around the world, and most of the world's long-lived extant lakes are affiliated with continental extensional basins. Lacustrine systems situated in the tropical latitudes commonly contain sediments that are exceptionally rich in organic matter because of a high biological productivity and, in some cases, prolonged bottom water anoxia (Demaison and Moore, 1980, Katz, 1990). Accordingly, modern tropical rift lakes are valuable sites for the study of the formation and concentration of oil and gas, especially because of the discovery of a considerable quantity of hydrocarbons on the Uganda margin of the Lake Albert Rift. The western rift valley of

[1]*Present address*: Geophysik GGD mbH, Leipzig, Germany.
[2]*Present address*: Department of Geosciences, University of Arizona, Tucson, Arizona, U.S.A.

Copyright ©2012 by The American Association of Petroleum Geologists.
DOI:10.1306/13291394M952903

the Cenozoic East African rift system (EARS) contains a string of ancient lakes that have been studied as modern analogs for lacustrine hydrocarbon systems in the rock record (Talbot, 1988; Katz, 1990; Scholz, 1995; Soreghan and Cohen, 1996). Lake Albert, the focus of this study, is the northernmost lake in the western rift valley, and unlike its southern counterparts, has been the subject of exploration activities for many years (Harris et al., 1956).

The EARS is commonly considered the classic example of continental breakup and extends more than 4500 km (2796 mi) from the Gulf of Aden to Mozambique (Figure 1). The western rift valley of the EARS contains some of the world's largest, deepest, and oldest lakes, which are home to numerous endemic floral and faunal species (Beadle, 1981). The sedimentary fills of these deeply subsided basins record long-term changes in environmental conditions in the tropics, in some instances at exceptionally high resolution (Johnson et al., 2002; Scholz et al., 2003). In addition, the lakes of the EARS provide reliable modern analogs for lacustrine hydrocarbon systems found in ancient rift basins, such as those buried offshore of Brazil and West Africa (Abrahao and Warme, 1990; McHargue, 1990). During the past approximately 70 yr, the Lake Albert rift valley (Figure 1) has received attention from petroleum geologists because of the presence of oil seeps, gas emanations, and hot springs along its flanks (Harris et al., 1956; Smith and Rose, 2002a, 2002b; Cassie et al., 2006). In the 1930s, several wells were completed along the basin's eastern margin, which encountered thick sections (>300 m [>984 ft]) of coarse-grained reservoir-facies sediments and sedimentary rocks but lacked economic quantities of hydrocarbons (Harris et al., 1956).

In 2003, renewed exploration interest in this region of the western rift resulted in a commercial marine-type seismic reflection survey on Lake Albert. This survey acquired 1650 km (1025 mi) of 24-fold digital multichannel seismic reflection data in a grid with approximately 3 km (1.9 mi) line spacing to image the synrift sediments accumulating in the basin. Using these new seismic reflection data, as well as new gravity modeling, and seismic correlations to existing deep exploration wells in the basin, we present a new high-fidelity view and detailed interpretation of the structure, stratigraphy, and basin evolution of the Lake Albert rift. In early 2010, the Ugandan Energy Ministry announced that the discovery made by Tullow Oil and Heritage Oil could amount to 6 billion bbl of oil.

## GEOLOGIC BACKGROUND

Lake Albert occupies the northernmost rift basin in the western rift valley. The lake is approximately 130 km (81 mi) long and approximately 35 km (22 mi) wide and is an open hydrologic system that receives its major input from the Semliki River to the southwest and the Victoria Nile to the northeast (Figure 1). Lake Albert is shallow by comparison with most other large East African rift lakes found to the south (e.g., lakes Tanganyika and Malawi), with a maximum water depth of approximately 58 m (36 mi) (Figure 2).

The western rift valley of the EARS is composed of a series of linked half-graben basins, many of which are currently occupied by large lake systems (Figure 1). Geophysical data and radiometric dating suggest that these basins probably formed beginning in the Miocene (Cohen et al., 1993; Nyblade and Brazier, 2002). No absolute age dates of the basal synrift lacustrine sediments have been recovered to date in any of the major western branch rift valley lakes. The ages of initiation of rifting have been estimated through the extrapolation of age-depth models in shallow cores (Cohen et al., 1993) or by dating of volcanic rocks adjacent to the large lakes (Ebinger et al., 1993), but in situ dating of deeply subsided and buried synrift deposits awaits future drilling efforts.

The basins commonly exhibit asymmetrical morphologies, with uplifted basin-bounding border fault margins opposing low-gradient flexural margins (Rosendahl, 1987). Half-graben basins in East Africa are typically 80 to 160 km (50–99 mi) long, 30 to 60 km (19–37 mi) wide, and may be linked end to end following along the axis of the rift valley (Rosendahl, 1987; Ebinger, 1989). In many instances, border fault segments of rift basins overlap in structurally complex regions known as accommodation or transfer zones (Rosendahl et al., 1986; Nelson et al., 1992). These zones link adjacent rift basins by accommodating differential strain between the tips of propagating normal faults and are observed in many extensional provinces worldwide, and are commonly entry points of coarse clastics (Scholz, 1995). Rift basin geometry and faulting patterns are probably influenced by deep-seated preexisting crustal heterogeneities (Versfelt and Rosendahl, 1989).

The Lake Albert rift is seismically active, and focal mechanism solutions support approximately northeast-southwest/east-west extension for the region (Nyblade and Langston, 1995), although extension direction may have rotated with time (Strecker et al., 1990; Ring et al., 1992). Lake Albert's watershed geology is made up of pre-Cambrian-aged metamorphic rocks, Karoo (Cretaceous) sedimentary rocks, and sequences of Neogene and Quaternary lacustrine and fluvial deposits. Unlike the Gregory rift, volcanism is not widespread in the western rift, although two small volcanic centers are present to the south of Lake Albert (Figure 1).

The geomorphology of the Lake Albert region has been shaped by deformation of the upper crust

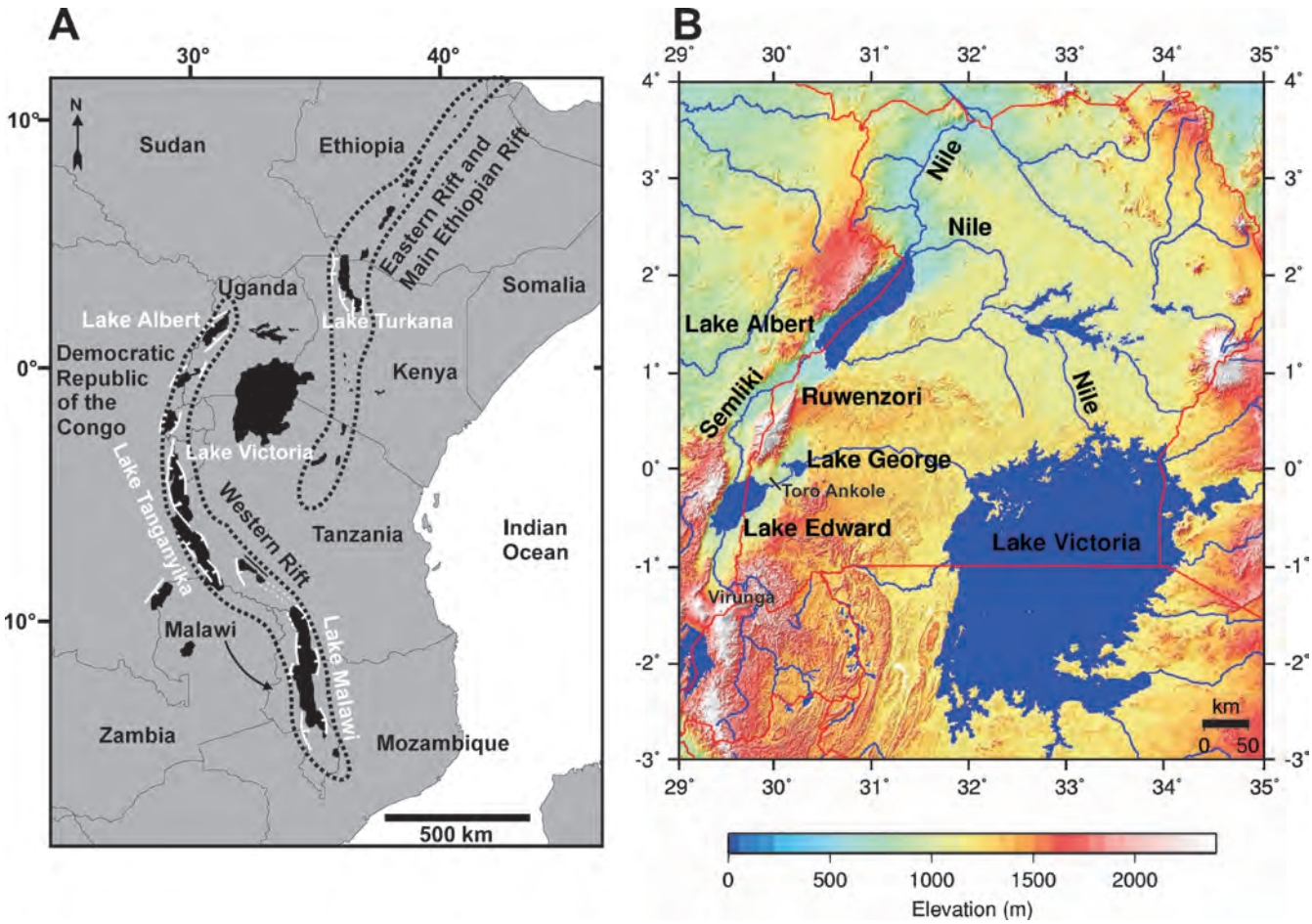


**Figure 1.** (A) East Africa with locations of major lakes, the Great Rift Valley and country boundaries. (B) Digital elevation model of East Africa. Note location of Lake Albert in the northern part of the rift valley. Virunga and Toro Ankole are volcanic complexes south of lakes Edward and Ruwenzori, respectively. 500 km (311 mi); 500 m (1640 ft).

associated with continental extension. Extension-related normal faulting produces significant topography, with the footwall blocks in some cases rising more than 2000 m (6562 ft) above adjacent rift basins. The Ruwenzori Mountains are a distinguishing landmark, and reach more than 4000 m (13,123 mi) above the adjacent Semliki Valley, the fluvial extension of the Albert rift basin (Figure 1). Surface uplift associated with the formation of the Albert and Edward rifts has also reversed several major drainage systems and helped contribute to the formation of lakes Victoria and Kyoga (Figure 1B) (Beadle, 1981).

Depositional patterns in lacustrine rift basins are strongly influenced by the half-graben basin morphology and its asymmetrical bathymetry (Frostick and Reid, 1989; Scholz et al., 1990; Soreghan and Cohen, 1996). Gross basin asymmetry and subsidence patterns commonly produce thick (>4 km [>2.5 mi]) wedge-shaped synrift sedimentary fills that thicken toward the border-fault margin (Morley, 1989). Uplifted rift shoulders divert major drainages away from the adjacent topographic depressions. As a result, border fault margins commonly display deep-water depositional processes characterized by gravity flows, fan aggradation, and organic-rich hemipelagic rain (Scholz et al., 1990; Soreghan et al., 1999). In contrast, flexural margin facies patterns are strongly influenced by littoral processes such as nearshore currents, waves, and prograding deltas, and may be zones of clastic sediment bypass (Tiercelin et al., 1992; Scholz et al., 1993; Scholz, 1995).

## METHODS

### Seismic Reflection Data Acquisition and Processing

The acquisition of the multichannel seismic (MCS) reflection data on Lake Albert occurred in 2003 using the

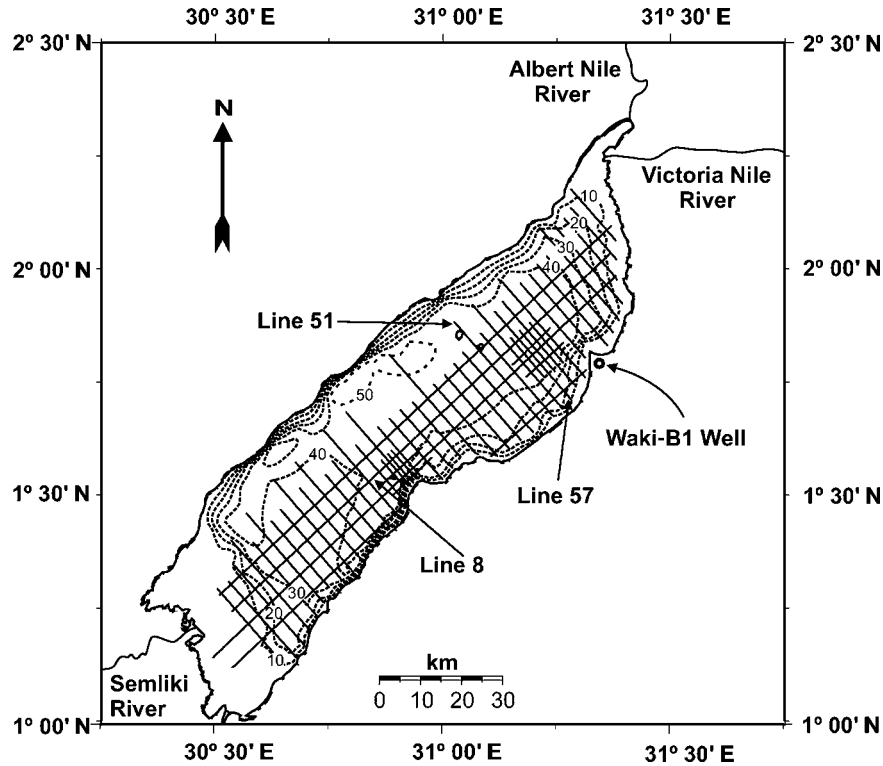


**Figure 2.** Bathymetry and multichannel seismic reflection track lines from Lake Albert. Note location of the Waki-B1 well on the northern part of the Ugandan (eastern) shore. Bathymetric data contributing to this map from work of Karner et al. (2000) and this study.

*Victoria III*, a converted fishing vessel. The survey was conducted along a grid of 46 dip and 9 strike lines (Figure 2), mainly covering the part of the lake in Ugandan territory. Positioning and shot stations were controlled by a Trimble differential global positioning system unit with submeter accuracy. An array of 3 bolt air guns, 0.66 L (40 in.) each, and a 1200 m (3937 ft) long digital streamer with 48 channels (25 m [82 ft] channel spacing) were used as the seismic source and receiver, respectively. Shot spacing was 25 m (82 ft), resulting in a 24-fold data set with a common depth point spacing of 12.5 m (41 ft). Source and streamer were generally towed at a depth of 3 m (10 ft), but brought closer to the surface where the water was very shallow (<10 m [32.8 ft]). The length of the recorded data is 6.144 s with a sampling rate of 1 ms.

Seismic data processing involved standard procedures, including spike and predictive deconvolution, bandpass filtering, normal move-out correction, stack, f-k migration, automatic gain control, and water bottom mute. Different parameters for the deconvolution and the bandpass filter as well as manually refined mutes were applied during the reprocessing, all of which were successful in suppressing multiple energy, except in the southern part of the survey area, where shallow biogenic gas was encountered.

The analyses of rift structures presented herein used a combination of the new offshore seismic reflection data, a reanalysis of existing gravity data augmented with bathymetric data, and for the onshore areas, Shuttle Radar Topography Mission (SRTM) 90 m (295 ft) Digital Elevation Model (DEM) data.

## Gravity Data Processing and Modeling

### Gravity Data Processing

Gravity data have been collected in the Albertine graben both onshore and offshore during the last several decades (Bullard, 1936; Upcott et al., 1996; Karner et al., 2000). An offshore survey was completed in 1992, greatly improving the gravity coverage of the rift valley. The data were used to (1) delimit the basin's border fault system, (2) estimate basin depth and sedimentary thickness, (3) determine sediment density, and (4) to model rift evolution (Upcott et al., 1996; Karner et al., 2000). In this study, we present a simple two-layer density model for the sedimentary infill of the basin. This model is not suitable for explaining the complete gravity signature of the basin, but it is able to provide a more robust framework for our seismic characterization of the deep basin structure.

The field of Bouguer anomalies as presented by Upcott et al. (1996) is part of the East African Bouguer gravity low (Bullard, 1936). The values away from the rift range from approximately −160 to −80 mGal and

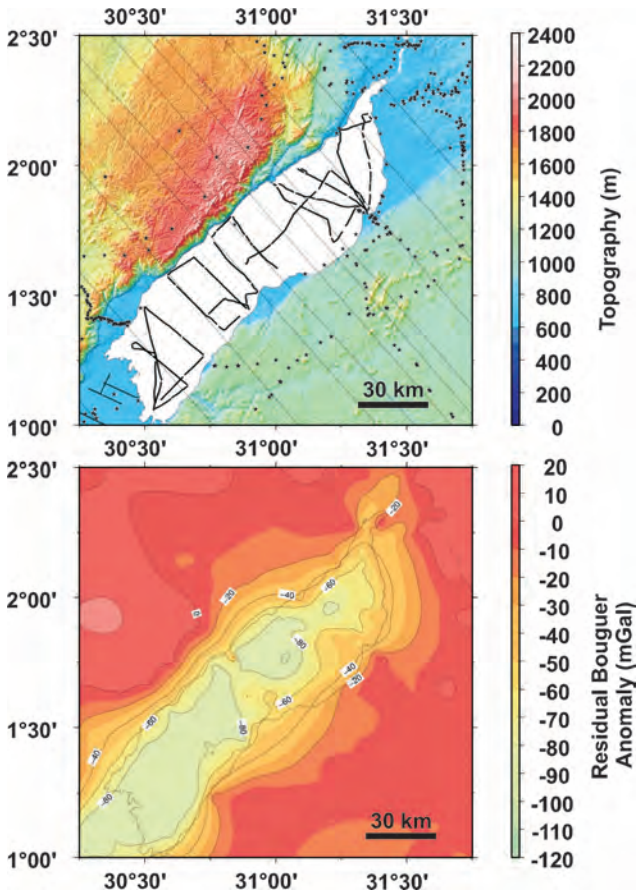


**Figure 3.** Digital elevation model of the Lake Albert region with gravity survey points (black dots) and northwest–southeast-trending cross sections that define the gravity model (top). Nine of the cross sections coincide with extrapolated seismic lines 1, 17, 31, 37, 45, 51, 55, 67, 79 (from southeast to northwest) and are complemented by two cross sections to the southwest and the northeast of the lake, respectively. The Residual Bouguer Anomaly (in mGal) of the Lake Albert region (bottom).

beneath Lake Albert from −225 to −160 mGal, with strong gradients at the rift valley margins.

To investigate the influence of the lake sediments on the gravity field, the regional trend of the Bouguer field was removed. This was completed by calculating a bicubic trend and subtracting it from the total field. The resulting field is herein referred to as the Residual Bouguer anomaly (Figure 3) and represents density anomalies of limited dimensions within the uppermost crust, consisting mainly of the rift valley infill.

### Gravity Modeling Approach

The goal of gravity modeling was to find a simple density model that is in agreement with the Residual Bouguer anomaly. The MCS data set was converted from time to depth using interval velocities derived from stacking velocities. The interpreted basement was picked in depth sections with a maximum basement depth of 5 km (3.1 mi) at the northwest end of line 51 (Figure 2). The basement depth was combined with the SRTM topography data along 11 parallel extrapolated lines (for location of lines, see Figure 3) to define the geometry of the rift valley. Bathymetry and topography data were used to fill the basin with water and sediment layers of appropriate thickness along each of the 11 lines.

For the forward modeling and inversion of densities, we interactively integrated gravity and magnetic data (Götze, 1978; Götze and Lahmeyer, 1988). The program uses triangulation between the 11 parallel lines to calculate three-dimensional (3-D) bodies and their combined gravity anomaly. By changing layer depth and/or density, observed and calculated fields are matched. The computed output results were also inverted to obtain density values.

In some areas on land, and especially in the vicinity of the mountainous and rugged rift flanks, gravity data points are sparse, and the triangulation computation fails to adequately interpolate the gravity influence of the elevated flanks. In addition, data on crustal structures and on densities outside the rift valley are not available. Accordingly, we used a constant background density of 2670 kg/m$^3$ for the subbasin basement and crustal rocks outside the valley, and set gravity anomaly values outside the valley to 0 mGal.

The Bouguer anomalies were calculated using reduction densities of 1000 kg/m$^3$ for the water column and 2670 kg/m$^3$ for the rocks between lake bottom and sea level (Upcott et al., 1996). Because no directly measured density data of the lake sediments are available, the model of sedimentary infill was limited to two theoretical layers: an approximately 600 m (1970 ft) thick layer (herein named the Bouguer block) extending from the lake bottom (~600 m [1970 ft] above mean sea level) to mean sea level, and the underlying sediments between mean sea level and basement. For both of these layers, constant densities were determined by inversion.

## Stratigraphy and Facies Analysis

Stratigraphic interpretations of both MCS data and early 20th century exploration well data relied on the principles of sequence stratigraphy (Van Wagoner et al., 1990; Bohacs et al., 2000; Scholz, 2001). Because of Lake Albert's unique stratal geometries, sequence boundaries were identified by sharp seismic facies transitions tied to unconformable facies associations in the Waki-B1 well (Figure 2). The well is located on the footwall

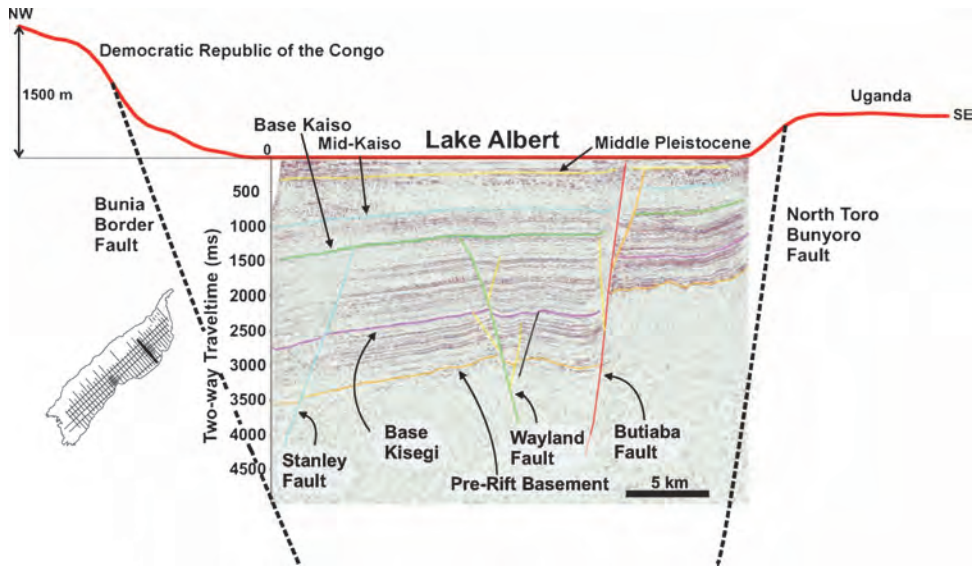


**Figure 4.** Multichannel seismic line 57 from the northern part of Lake Albert (see track line inset for location). Red line at surface of profile indicates regional topography.

block of the Butiaba fault, approximately 5 km (3.1 mi) from the nearest seismic profile. Although this is a projection to the nearest line, the footwall block is relatively undeformed to the south, as observed on numerous seismic images (Figure 2). Because this well was drilled more than 60 yr before the acquisition of the seismic data, no downhole velocity surveys are available for specific correlation of the well data to the seismic records.

## RESULTS AND INTERPRETATIONS

### Structural Observations from Seismic Reflection and Shuttle Radar Topography Mission 90 m (295 ft) Digital Elevation Model Data

The Lake Albert rift is a symmetrical full graben, bordered on the northwest by a steeply dipping planar fault, and on the southeast by a complex of steeply dipping faults. The base of the section and top of synrift basement is clearly identified and is nearly flat lying, as are the bulk of the reflections of the synrift strata (Figures 4, 5). Accordingly, it appears that both sets of boundary faults were continuously active throughout the history of the rift.

The western margin of Lake Albert is bounded along its length (~130 km [~81 mi]) by the Bunia border fault, which strikes approximately N40° to 60°E (Figure 6). Footwall uplift on this basin-bounding structure produces significant topography adjacent to the lake, with elevations of the Blue Mountains of the Democratic Republic of the Congo reaching a maximum height of approximately 1650 m (~5413 ft) above modern lake level (Figure 1B). Seismic reflection data acquired on the hanging-wall block adjacent to this border fault indicate that the location of maximum subsidence in the basin is situated in the northern part of the lake (Figure 6). Maximum depth to crystalline basement reaches approximately 4100 ms two-way traveltime (TWTT) in this locality and is filled almost entirely with synrift sediments (Figure 4).

The southeastern shore of Lake Albert is structurally complex, and deformation of the upper crust in this area has influenced drainage patterns and delivery of sediment to the basin floor of the Albert rift. Several large lineaments are observed in the SRTM DEM, including the northern Toro Bunyoro Fault and the Tonya Fault (Figure 6). The trace of the northern Toro Bunyoro Fault (Upcott et al., 1996) is a 90 km (56 mi) long onshore lineament that trends N40° to 60°E. The northern Toro Bunyoro Fault produces an escarpment east of the modern lake surface in the northern half of Lake Albert that rises approximately 400 m above the lake. The Waki-B1 Well was drilled into a hanging-wall anticline adjacent to this structure.

The Tonya Fault is a down-to-the-west basin border fault that strikes approximately N20° to 35°E and extends for approximately 85 km (~53 mi) along the southeastern shore of Lake Albert (Figure 6). Whereas the Tonya Fault produces a sharp onshore escarpment rising approximately 600 m (~1970 ft) above lake level at its highest point, seismic reflection data indicate that the zone of normal fault deformation also extends offshore (Figure 6). Maximum observed displacement on prerift basement offshore on the hanging wall of the Tonya Fault is approximately 2000 ms TWTT (Figure 6). The northern tip of the Tonya Fault terminates in a

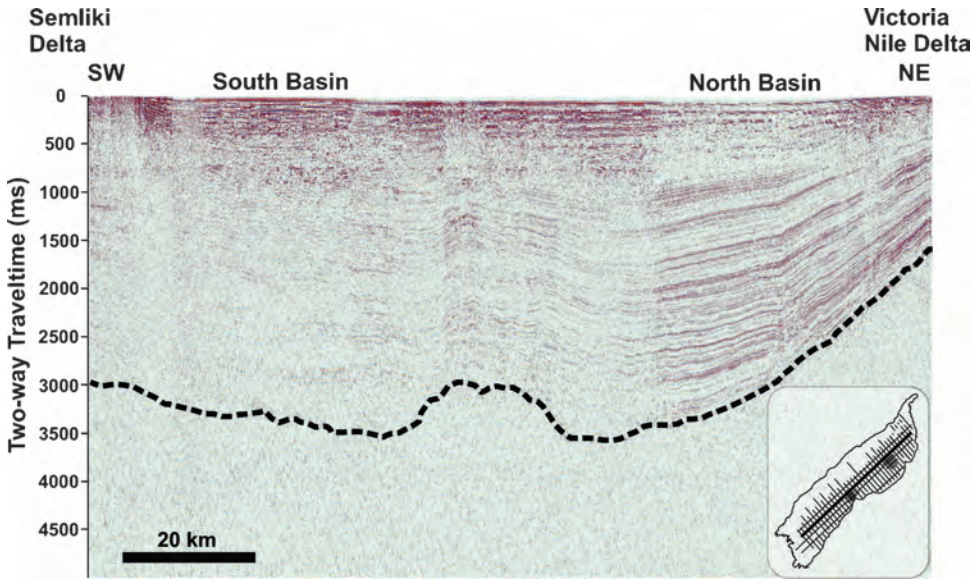


**Figure 5.** Lake Albert multichannel seismic profile HLA8 that extends along the length of the basin (see track line map inset). Prerift basement shallows and the sediment section thins markedly to the north. To the south section extends on to the Semliki River plain. Note two distinct basins in north and south.

region of complex deformation near the center of the lake. At the basin scale, a large relay ramp is observed, which developed through the interaction of the northern Toro Bunyoro and the Tonya faults (Figure 6). Several minor normal faults synthetic to these larger structures are present in the region of overlap, as is the Howa River channel and several Quaternary Kaiso outcrops studied by Bishop (1969). Offshore, deformation consists of normal faults synthetic to the Tonya Fault, although these are confined to an area close to the eastern shore (Figure 6). The prerift basement is much shallower in this transition zone, ranging between 2800 and 3400 ms TWTT on the Tonya Fault hanging wall (Figure 6).

South of the transition zone, the signal-to-noise ratio in the seismic data is reduced and is likely a result of shallow gas in modern sediments. Accordingly, intrabasinal faults are not readily observed south of the transition zone. To the north, the most significant fault observed in the seismic data is the Butiaba Fault, located approximately 12 km (~7.5 mi) off the eastern shore of the lake (Figure 6). The Butiaba Fault is approximately 75 km (~47 mi) long down-to-the-northwest normal fault that strikes N40° to 60°E. The Butiaba Fault is a planar structure, dipping steeply at approximately 40°. The footwall of the Butiaba Fault creates an uplifted littoral platform along the eastern shore of the lake, where water depths are less than 35 m (115 ft) (Figure 2). Displacement on prerift basement in the Butiaba Fault hanging wall reaches a maximum of approximately 1600 ms TWTT near the center of the fault (Figure 4). The maximum basement depth on the hanging wall adjacent to the Butiaba Fault is approximately 3600 ms TWTT (Figure 6).

## Structural Observations from Gravity

The Residual Bouguer anomaly is negative with a minimum of −100 mGal in the center of the lake. It is very smooth (~−80 mGal) in the southern lake basin and

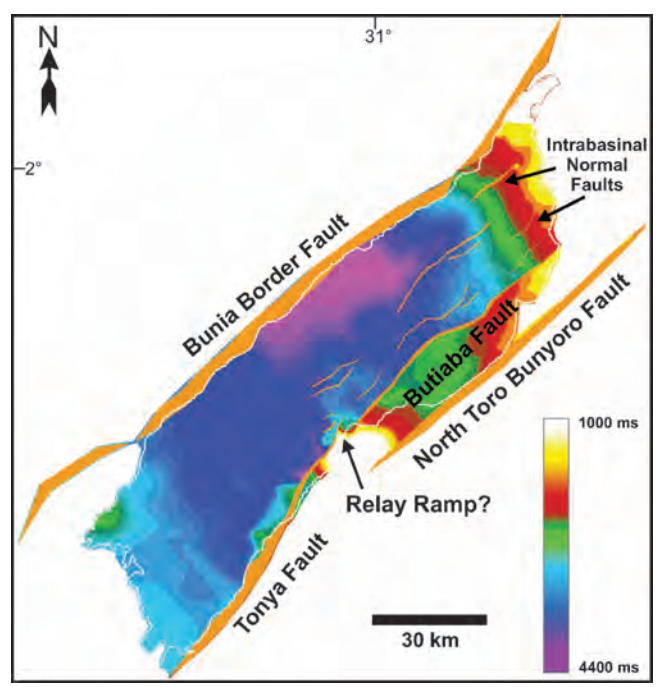


**Figure 6.** Structure contour and fault map on prerift basement. Note that main depocenter is located on the northwestern side of the basin, adjacent to the main basin boundary fault. A rider block with a thinner sedimentary section is observed adjacent to the boundary fault system on the Ugandan side of the lake in the northeast.

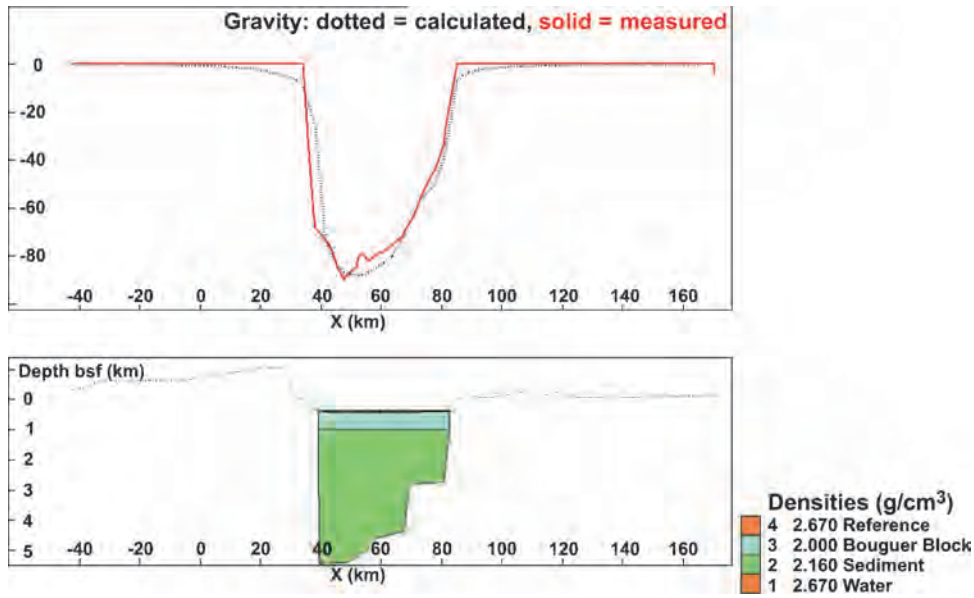


**Figure 7.** Cross section of the gravity model of Lake Albert along line 51 (bottom) and corresponding calculated (dotted) and observed (solid red) gravity curves (top). Crustal rocks outside the rift valley and the lake water are excluded from gravity calculations by setting their density to the background value of 2.67 g/cm$^3$.

shows more variation in the northern part. Along the coastline of the lake, the anomaly is on the order of −20 to −50 mGal.

To constrain some of the structural observations from the MCS data, the Residual Bouguer anomaly was inverted for the densities of rift basin sediments. We inverted for the densities of the Bouguer block (~600 m [~1970 ft] thick block of sediments between the lake floor and mean sea level) and the underlying block of rift valley sediments. The average densities are calculated to 2000 (±80) kg/m$^3$ and 2160 (±20) kg/m$^3$, respectively.

These density values are in good agreement with density estimations based on free-air gravity anomalies published by Karner et al. (2000). Their model results in slightly higher density values that is a direct consequence of the use of the free-air gravity anomaly, which includes the gravity influence of the masses above sea level. The effect of these masses is removed from the Bouguer anomaly, which is therefore more negative than the free-air anomaly and requires lower sediment density values within the rift valley. The maximum basin depth estimation of 5 km (3.1 mi) presented by Karner et al. (2000) is identical with the values computed from depth converting the MCS lines.

Figure 7 shows a cross section example from seismic line 51. The lower frame shows topography (dotted line) from northwest to southeast and the modeled water, Bouguer, and sediment layers inside the valley. The upper frame shows good agreement between calculated (dotted) and observed (red solid line) Bouguer gravity.

Figure 8 shows a map view of the difference between observed and calculated Bouguer anomalies and a histogram of these differences. The correlation between the anomalies is very high ($r$ = 0.96). The map indicates that a difference of less than ±5 mGal exists between the observed and the calculated field across the entire lake. Considering the simplified density model (without density gradient) and lacking real density values, this represents a good first-order approximation. The density model suggests the basin's division into two subbasins. In the southern subbasin, the mismatch between calculated and observed gravity anomalies is only on the order of a few mGal (Figure 8). In the northern subbasin, some localities exist where the modeled density is too low (blue colors) or too high (red colors).

The two blue regions indicate areas where the observed Bouguer anomaly is less negative than the calculated curve. This could be compensated for by higher uplifted basement or by higher sediment densities in the model. Although slight basement dips are observed toward the northwest, these depth differences are not sufficient to cause the observed relative gravity highs, and increased sediment densities in these areas are also problematic. Second, another hypothesis, which was not modeled, is that sediment densities are lower, which generally implies lower seismic velocities. This would generate a considerably shallower basement than calculated and the integrated effect would be a calculated anomaly that is less negative. A third explanation is basement faulting that occurs in the blue areas (Figure 8). The most likely reason for the gravity mismatch is a combination of complicated basement topography, including the relay ramp, and a high spatial variability of physical sediment properties that is beyond the resolution of the simple two-layer model.

The central red region between the two blue areas indicates that the modeled gravity curve is not sufficiently negative. This could be corrected by a slightly

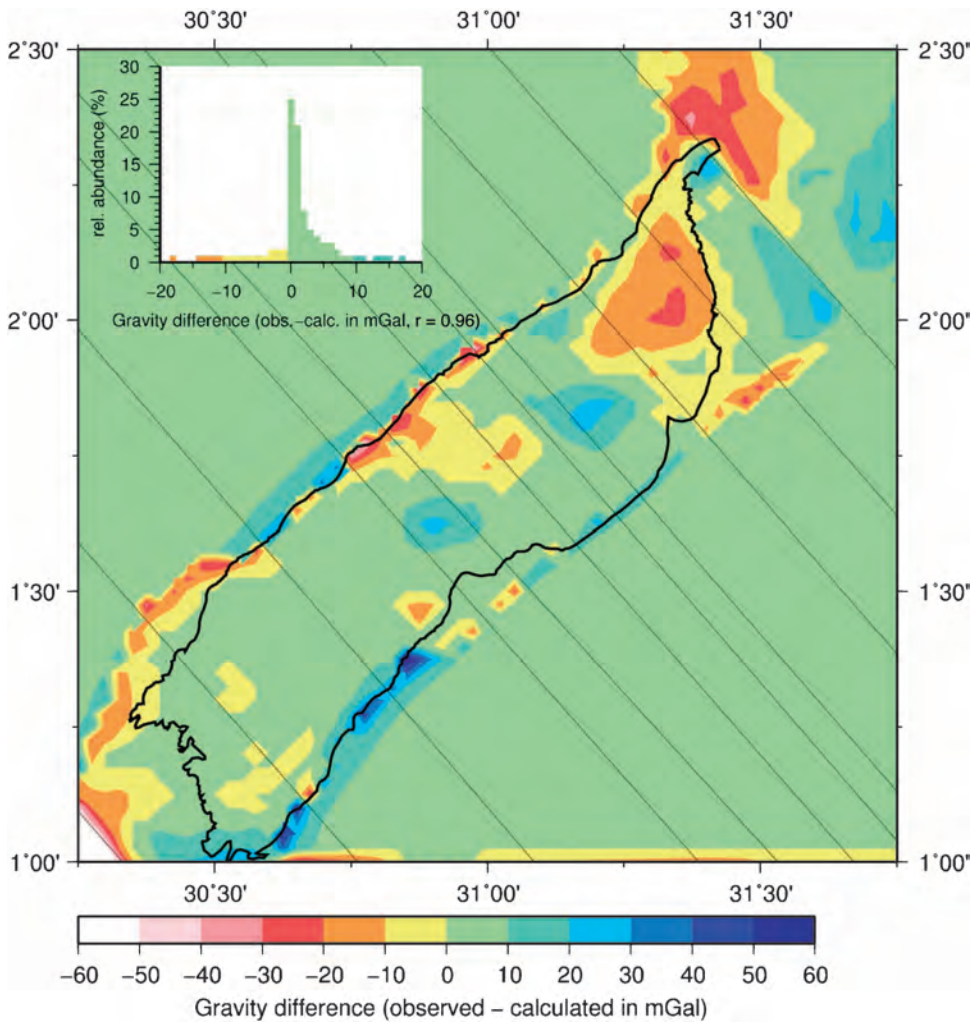


**Figure 8.** Difference between calculated and observed gravity fields of the Lake Albert region and (inset) relative abundance of difference values.

lower sediment density (−40 kg/m$^3$), by a deeper basement estimate (~300 m [~984 ft]), or by a moderate adjustment of both of these parameters.

In the northernmost part of the lake, the red colors of Figure 8 also indicate that the modeled gravity is not sufficiently negative. This could be compensated for by lower sediment densities than average. A good match of observed and calculated gravity for this area can be achieved with densities of 1850 and 2050 kg/m$^3$, respectively. An explanation for these lower density values includes shallow gas-bearing sediments, which are also suggested by the low signal-to-noise ratio of the seismic data in this area. The Nile River inflow is close to this region and is a likely source of terrigenous organic matter that may be responsible for generating biogenic gas in the shallow subsurface of this part of the lake.

The Residual Bouguer anomaly and the gravity modeling results suggest that the basin is separated into two subbasins. In addition, the close approximation of observed gravity values in the southern subbasin to a simple two-layer model confirms the seismic interpretation of a flat and mostly unfaulted subbasin containing sediments of uniform density. The northern subbasin, however, exhibits a more complex eastern margin boundary fault and more complex structures that inhibited laterally uniform sediment distribution. Accordingly, the high variability of observed density in this area cannot be readily explained by a simple two-layer model.

## Stratigraphic Observations from Seismic Reflection Data

Five stratigraphic packages were interpreted in the basin from the MCS data set, which are each bounded by key chronostratigraphic surfaces identifiable on seismic profiles and in the Waki-B1 stratigraphic log (Harris et al., 1956). These surfaces, from oldest to youngest, are (1) prerift basement, (2) base-Kisegi, (3) base-Kaiso, (4) mid-Kaiso, and (5) middle Pleistocene surfaces (Figure 4; Table 1).

## Prerift Basement

Prerift basement is distinguished by a wavy, two- to three-cycle, low-frequency reflection package. Beneath the prerift basement reflections, the seismic response is low amplitude and internally chaotic. Locally, reflections lap onto the basement surface, although on many dip profiles, reflections simply drape the prerift basement (Figure 4). Prerift basement correlates with crystalline rocks at the base of the Waki-B1 well more than 1189 m (3900 ft) below the surface (Figure 9). The seismic character of the lowermost strata just above the basement reflections is defined by variable amplitude, variably continuous or discontinuous reflections, with local reflection-free zones. These reflections correlate with sandstone and conglomerate beds in the Waki-B1 well, which taken together are approximately 12 m (~39 ft) thick.

High-amplitude continuous reflections typify most of the stratigraphic sections above prerift basement and the earliest synrift strata. This package of reflections correlates with shoaling-upward parasequences measured on the Waki-B1 lithology log composed of organic-rich shale bedsets capped by thin beds of sandstone (Figures 4, 10, 11). These parasequences range in thickness between 6 and 64 m (20 and 210 ft). Stacked kerogen-rich shale beds dominate in Waki-B1 below the base-Kisegi surface, reaching a maximum thickness of approximately 58 m (~190 ft). The stratigraphic section between prerift basement and the base-Kisegi surface is approximately 228 m (~748 ft) thick.

## Base-Kisegi

The base-Kisegi surface is a high-amplitude, continuous, low-frequency reflection in the lower part of the section (Figures 4, 10, 11). This surface correlates to a thick (~15 m [~49 ft]) conglomerate bed overlying a thinner organic-rich shale bed in the Waki-B1 well. The seismic stratigraphic package above the base-Kisegi surface is commonly distinguished by high-amplitude variable-frequency parallel reflections. Overlying the base-Kisegi surface in Waki-B1 are numerous upward-shoaling parasequences composed of thickly bedded and massive sandstones interbedded with thin organic-rich shale beds (Figure 11). Sandstone bed thickness encountered in the Waki-B1 well reaches a maximum of approximately 30 m (~98 ft) approximately 885 m (~2900 ft) beneath the surface. A clear lithofacies transition occurs in the well approximately 200 m (~656 ft) above the base-Kisegi surface, where sandstone beds become less prevalent in favor of moderately thick parasequences composed of many stacked shale beds. Up section, another transition occurs in the well at 685 m (2247 ft) below the surface. Here, thin and medium sandstone beds are observed in the Kisegi interval and, in some instances, include evidence of sedimentary pyrite. Lithologies approaching the overlying base-Kaiso surface are dominantly fine-grained siliciclastics (Figure 11). The stratigraphic section between the base-Kisegi and base-Kaiso surfaces is approximately 431 m (~1414 ft) thick.

## Base-Kaiso

The next key surface identified in the seismic data set is termed the base-Kaiso surface (Table 1). The base-Kaiso surface is the most prominent and continuous reflection in the entire northern part of the rift basin (Figure 11). We correlate this to a greater than 25 m (>82 ft) thick carbonate-cemented sandstone interval observed in the Waki-B1 well (Figure 11). The seismic stratigraphic section above the base-Kaiso surface is markedly less continuous, with more variable amplitudes than those observed in the lower part of the section (Figures 4, 10). Several transparent zones are evident, and high-frequency reflections are wavy. In addition, strong lateral variations in seismic character are present above the base-Kaiso surface. For example, discontinuous reflections are common along the western margin of the basin, whereas reflections near the Butiaba platform are characterized by high amplitudes and high continuity (Figure 10). Lithofacies in the Waki-B1 well coincident with this interval are dominantly organic-rich shale and clay. Parasequences are indistinct and thicker above the base-Kaiso surface because of a limited number of coarse siliciclastic beds. Where they do occur, sandstone and conglomerate beds are thin (<3 m) and are either ferruginous or calcareous. In contrast, thicker stacked beds of clay and shale are common above the base-Kaiso surface (Figure 9). The stratigraphic section between the base-Kaiso and the overlying mid-Kaiso surfaces is approximately 189 m (~620 ft) thick.

## Mid-Kaiso

The next significant surface mapped in our study is the mid-Kaiso surface (Figures 4, 10; Table 1), manifested locally on the Butiaba footwall as a moderately continuous high-amplitude reflection. In the deep basin, the mid-Kaiso surface marks the boundary between a low-frequency discontinuous reflection package and a high-frequency discontinuous package (Figures 4, 10). We correlate this boundary to several thin to moderately thick conglomerate beds overlying an organic-rich

**Table 1.** Stratigraphic summary.

| Unit/Surface Name | Relative Age | Seismic Character | Lithology (Waki-B1 Well Correlation) | Facies Interpretation |
|---|---|---|---|---|
| Recent unit | Late Pleistocene | Continuous reflections offshore; discontinuous in proximal areas | Uppermost Kaiso beds and big sand; organic-rich muds offshore | Dominantly shallow lacustrine in basin; alluvial in proximal areas |
| Middle Pleistocene | Middle Pleistocene? | Base of reflective section | Lignitic and shelly sandstones | Alternating shallow lacustrine/wetland/ savannah landscape |
| Unit 4 (above Green) | Late Synrift | Discontinuous in west, moderately continuous in east | Thick packages of conglomerate and sandstone; upper Kaiso beds | Alluvial/fluvial conditions |
| Mid-Kaiso | Early Pleistocene? | Moderately continuous, high-amplitude reflection | Thick sandstone | Shallow lacustrine in east; stacked fluvial in rapidly subsiding west |
| Unit 3 (above mm 25) | Middle Synrift; early Pleistocene? | Alternating continuous, high-amplitude reflections with discontinuous/transparent packages | Alternating thin calcareous shale/ siltstone packages; lower Kaiso beds | Alternating playa lacustrine and fluvial conditions |
| Base-Kaiso | Pliocene–Pleistocene boundary???? | High-amplitude, very continuous; most prominent reflection in basin | $CaCO_3$-cemented sandstone | Correlates to carbonate-cemented sand in Waki-B1 well; prolonged low-lake stage/desiccation surface |
| Unit 2 (above purple) | Early–middle synrift: Pliocene?? | Parallel, high-amplitude, continuous reflections; overall very bright, high-amplitude continuous reflections | Bulk of section is organic-rich lacustrine shale Kisegi beds | Deep lake phase; dominantly open lacustrine environment with episodes of lake desiccation producing hardgrounds, evaporite sequences or paleosols |
| Base-Kisegi | Miocene/Pliocene boundary???? | High-amplitude, very continuous | Thick conglomerate | Correlates to interpreted base of Kisegi Fm in Waki-B1 well; sand with pebbles; probably represents a major desiccation surface |
| Unit 1 | Early rift: Miocene–early Pliocene?? | Variable amplitudes, reflection free and discontinuous reflections | Dominantly organic-rich lacustrine shale; Alluvial wash at base; Miocene beds | Fluvial alluvial/shallow lacustrine?; correlates to basal conglomerate in Waki-B1 well; grades into organic-rich lacustrine shale |
| Prerift Basement | Precambrian | Wavy, irregular, ~2- to 3-cycle low-frequency, moderately continuous reflection package | Crystalline basement/prerift surface | Rift initiation during Miocene, or possibly early Pliocene time? |

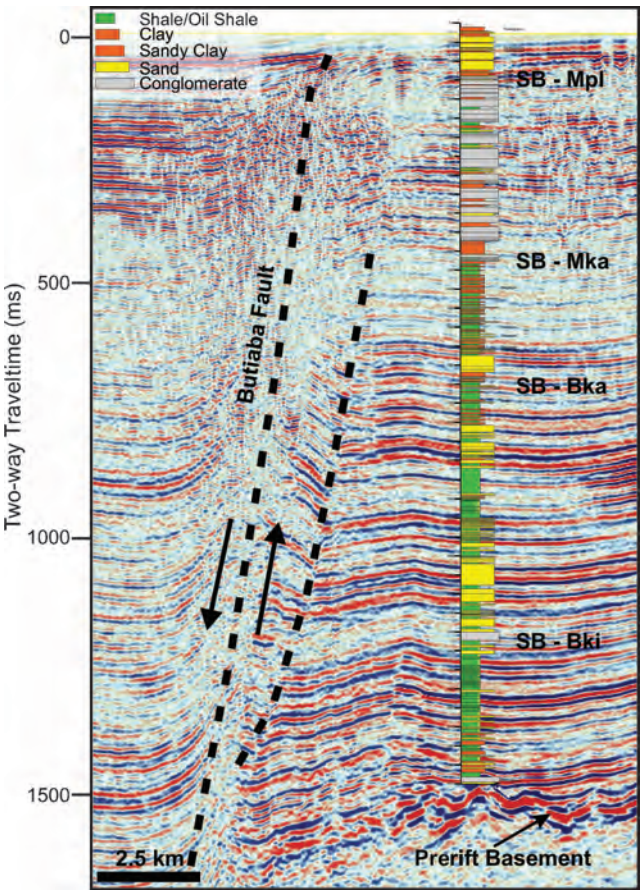


**Figure 9.** Eastern part of seismic line 57, showing reflections of the uplifted Butiaba Fault footwall. Throughout the basin, the high-amplitude prerift basement event overlies chaotic low-amplitude reflections of crystalline basement. The Waki-B1 lithostratgraphic log is projected onto the seismic section from less than 15 km (9.3 mi) away. Note the significant vertical changes both in the well stratigraphy and in seismic facies characteristics. The overall coarsening-upward motif of the Waki-B1 well is interpreted to reflect fluctuating depositional environments responding to periods of climatic and tectonic flux since the Miocene. SB = sequence boundary; Bki = Base Kisegi; Bka = Base Kaiso; Mka = Mid-Kaiso; Mpl = Middle Pleistocene. 2.5 km (1.5 mi).

shale bed, approximately 375 m (~1230 ft) below the surface in the Butiaba Waki-B1 well (Figure 11). Above the mid-Kaiso surface in the northern part of the rift, we observe a distinct high-amplitude package of high-frequency and continuous reflections, which is especially prevalent in the center and eastern part of the Butiaba hanging wall (Figures 4, 10). At the same stratigraphic interval in the far northwest of the basin, the continuous reflection packages grade into less continuous seismic facies. These seismic stratigraphic packages correlate with indistinct parasequences in the Waki-B1 well. Near the mid-Kaiso surface, thick conglomerate units are interbedded with clay beds of variable thickness. Parasequence thicknesses are on the order of 9 to 30 m (30–98 ft). Up section, thin beds of organic-rich shale are capped by thicker beds of conglomerate. Just below the middle Pleistocene surface, lithofacies in the well appear similar to those near the mid-Kaiso surface. The stratigraphic section between the mid-Kaiso and middle Pleistocene surfaces is approximately 288 m (~945 ft) thick.

### Middle Pleistocene

Near the top of the stratigraphic section (~200 ms) is the middle Pleistocene surface, which is defined as the top of the highly reflective, high-frequency, continuous interval above the mid-Kaiso surface. This reflection is a high-amplitude, lower frequency, continuous event that we observe across the entire basin (Figures 4, 10). The transition between lignite-rich conglomerate beds and shell-rich sandy claystone marks the middle Pleistocene boundary in Waki-B1. Above the middle Pleistocene surface, we observe a low-reflectivity transparent unit, approximately 100 ms in thickness, which extends to the modern lake floor. Lithofacies above the middle Pleistocene surface in Waki-B1 include thick beds of sandstone interbedded with shelly sand-rich claystone beds. Parasequences are difficult to interpret above the middle Pleistocene surface because flooding surfaces are not readily apparent.

High-resolution subbottom images of the stratigraphic section reveal a shallow basinwide unconformity marked by the onlap of low-amplitude reflections onto high-amplitude continuous sets of reflections less than 100 ms below the modern lake floor. The thickness of the uppermost stratigraphic unit varies along strike, thinning and lapping onto structural highs in the north and thickening greatly into a 90 $km^2$ (35 $mi^2$) lens before being truncated by faults in the south (Figure 10). The sedimentary lens forms a bathymetric high where water depth does not exceed 35 m (115 ft); seismic reflections offlap the feature bidirectionally toward the north and south.

## DISCUSSION AND INTERPRETATIONS

### Structure

Lake Albert's basin geometry is a relatively simple full-graben structure, with a paired boundary fault and rider block feature on the southeastern margin of the basin and a single dominant normal fault system on the northwestern margin (Figures 4, 6). Full-graben systems

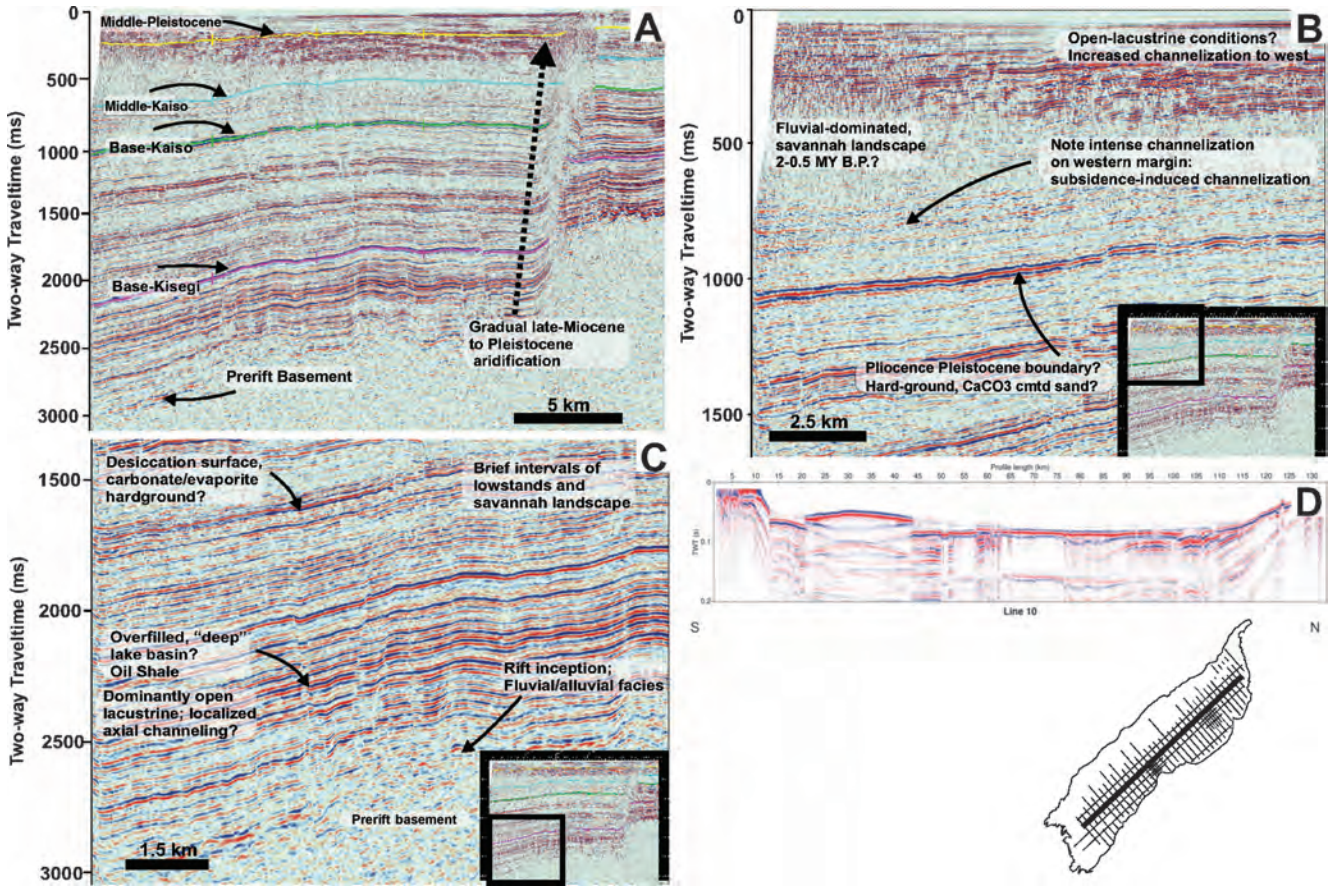


**Figure 10.** Seismic facies interpretation of line 57 (A), with adjacent panels from this line (B, C) illustrating detailed seismic facies variability, and overall, long-term change from wet, open, and possibly deep lacustrine conditions in the Miocene, to dryer and shallower lacustrine and fluvial environments in the Pleistocene. Panel D shows the reprocessed upper part of axial line 8, from the Semliki Delta (S) to the Nile outlet (N). See text for discussion.

are not encountered elsewhere in the western rift valley. For instance, fault patterns observed in the Lake Albert rift are unlike those observed in Lake Tanganyika, where initial models of continental extension were developed (Reynolds and Rosendahl, 1984; Rosendahl et al., 1986; Morley, 1988; Rosendahl et al., 1988). Commonly, a single bounding border fault controls basin architecture and is opposed by a flexural or shoaling margin created by hanging-wall collapse. In the case of Lake Albert, a single bounding border fault is observed on the western margin of the basin, but it is opposed on the eastern margin by a distributed border fault complex composed of several major faults situated both onshore and offshore (Figures 4, 6). This fault geometry produces two structural subbasins. Similar amounts of displacement on the Bunia and Butiaba faults produce a near-horizontal prerift basement in northern Lake Albert, with a dip to the west of less than 1°. Maximum synrift sedimentary thickness in the northern basin is approximately 4000 ms TWTT, whereas maximum sediment thickness on the footwall block of the Butiaba platform is approximately 2600 ms TWTT.

Several basement-involved secondary normal faults deform the synrift section in the northern subbasin, and these may be responsible for the complex output of the gravity model developed in this area. Displacements on these second-order faults are locally up to approximately 100 ms TWTT. Among the largest of these faults, herein named the Wayland Fault, is approximately 28 km long east-facing normal fault antithetic to the Butiaba Fault (Figure 4). This fault occurs approximately 18 km (~11 mi) from the eastern shore, and it has a strike of N40° to 60°E. Maximum displacement on the Wayland Fault is approximately 45 ms TWTT. Two small down-to-the-west fault splays on the Wayland Fault's hanging-wall block create small rollover features that may be effective hydrocarbon traps. Another large basement-involved secondary fault, herein named the Stanley Fault, is located approximately 14 km (~9 mi) from the western lake shore. The length of the Stanley Fault

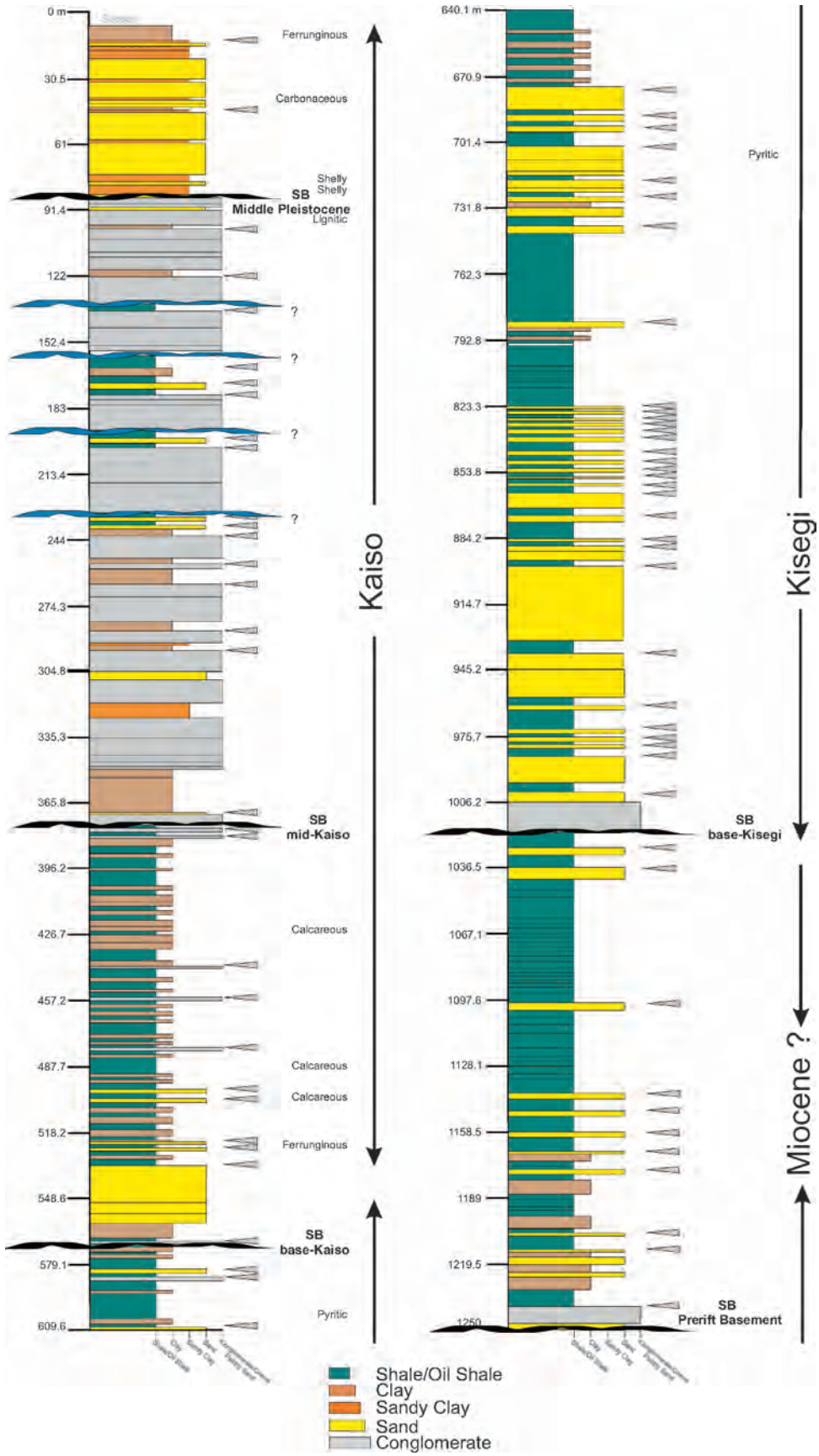


**Figure 11.** Detailed lithology log of the Waki-B1 well (modified from Harris et al., 1956). Depth increments are given in meters. Relative grain size is expressed by the length of horizontal beds (ranging from oil shale to conglomerate). The well is shown with sequence-stratigraphic interpretations. Small triangles mark the locations of interpreted parasequences boundaries or flooding surfaces. Ribbons mark the locations of interpreted sequences. The overall coarsening-upward trend in the well reflects major changes in lake hydrology since the Miocene, likely responding to changes in regional precipitation patterns. See text for explanation.

segment is approximately 34 km (~21 mi) long, and it strikes approximately N40° to 60°E. The maximum displacement on this fault is approximately 170 ms TWTT. The Stanley Fault is antithetic to the Bunia border fault, and the interaction of these faults helps to form the region of thickest sediment accumulation in the northern subbasin.

## Stratigraphy

Basin subsidence is accommodated roughly equally on both sides of the basin, hence, the relief within rift valley proper is minimal, and the overall stratigraphic geometry is of flat-lying or draping reflections from the bottom to the top of the section (Figure 4). Such a low-relief geometry is in strong contrast to most of the other large rift lake basins of the western rift valley, whose structural domains are mainly characterized by highly asymmetrical half-graben basins (Rosendahl, 1987; Scholz et al., 1989). Most of the half-graben basins that comprise the Lake Tanganyika and Lake Malawi rifts demonstrate clear wedge-shaped stratigraphies, and in some localities, contain pronounced incised valleys or subaqueous canyons (Scholz et al., 1990). Accordingly, we interpret the early landscapes of the Albert rift valley to have been dominated by a flat valley floor that was periodically flooded to varying degrees.

Pronounced angular unconformities define depositional sequence boundaries in many rift basins on account of asymmetrical subsidence patterns and rapid changes in the development of potential accommodation (Gawthorpe and Leeder, 2000). Such marked angular relations are not observed in the Lake Albert seismic data, except on very limited local scales. Classical sequence boundaries are thus less obvious in this basin, at least on a scale of our deep basin MCS data set. Although discrete termination relations do not readily define basinwide sequence boundaries in the Albert rift, marked vertical and lateral variations in seismic facies exist that help distinguish variability in depositional conditions throughout the basin's history. Sequence boundaries and parasequences are much easier to constrain using the lithofacies stacking patterns in the Waki-B1 well. Sudden transitions from organic-rich shale beds to coarse conglomerates likely represent important climatic or tectonic events that juxtapose profundal and supralittoral lake plain or alluvial depositional environments, marking potential sequence boundaries. Parasequences, the sedimentary building blocks of sequences, are genetically related packages of sediment that are defined by flooding surfaces, marked by the profundal sediments overlying coarser littoral or supralittoral sediments (Van Wagoner et al., 1990; Bohacs et al., 2000). Our methodology for interpreting Lake Albert's stratigraphic framework relies on identifying stratigraphic surfaces identifiable in both seismic and well log records. Although the method provides the most robust stratigraphic interpretation for the basin, it is important to emphasize several assumptions when correlating regional-scale data sets with different resolutions. The process of integrating well data with seismic lines and making jump ties between widely spaced data points is not uncommon studies of frontier basins. Because the development of sequence boundaries notionally requires a fundamental change in the environmental conditions impacting a sedimentary basin, the sequence boundaries interpreted on the Waki-B1 well must be present in the stratigraphic record underlying the extant lake. The projection of the well record onto the nearest seismic line suggests that several of the high-amplitude reflections that are prominent in the seismic section provide a plausible correlation to interpreted sequences in the well. This is especially true for the base-Kisegi and base-Kaiso boundaries (Figure 5). Picking other boundaries required more interpretation and ultimately focused on clear vertical changes in seismic facies. This process is complicated by (1) an increase in lateral facies variability moving down depositional dip and (2) the presence of the Butiaba Fault, which demands an additional correlation from the platform to the basin. As a consequence, the interpretations we present here are conservative, mainly reflecting wholesale changes in the lake's depositional mode through time.

Above prerift basement, we interpret the earliest synrift strata to represent fluvial and fluvial-lacustrine sediments. Fluvial deposits are commonly observed at the base of many rift sections (Lambiase, 1990), and a modern analog of this environment may be the Okavango delta of Botswana and South Africa, where early extensional subsidence is currently underway (Modisi et al., 2000). The Okavango delta is a region of ephemeral lakes, swamps, and wadis that fill and desiccate on a seasonal basis. Rift margin topography was likely minimal during the initial stage of Albert Graben development. Most of the stratigraphic package above the lowermost fluvial/alluvial sequence is composed of highly reflective, high-amplitude, and continuous reflections, which we interpret as dominantly organic-rich shale deposited in an open lacustrine environment. This interpretation is confirmed in the Waki-B1 stratigraphy. Adjacent to prerift basement, parasequences are thin and appear weakly aggradational, which we interpret to reflect basin infilling during a period of low lake level as the basin is established. At about 1110 m (~3642 ft) depth in the Waki-B1 well, parasequences are observed to be thicker (>40 m [>131 ft]) than underlying strata and are characterized by stacked beds of oil shale, which strongly suggest deposition in the profundal

environment. These parasequences record a major transgression in the basin and suggest the establishment of a large deep lake that may have experienced extended periods of bottom-water anoxia.

Correlation of the seismic reflection data to the Waki-B1 well suggests that the overlying base-Kisegi surface correlates to the Miocene-Pliocene boundary (Harris et al., 1956). At present, no available data exist to assess the accuracy of this age assignment of Harris et al. (1956). Lithologically, the surface correlates to a conglomerate bed overlying a shale bed identified in the well and is indicative of a desiccation event or alluvial surface present in the basin at this time (Figure 11). The base-Kisegi surface must represent a prolonged and severe desiccation event that produced the distinctive and highly reflective surface.

The thick sedimentary section between the base-Kisegi and overlying base-Kaiso surfaces consists of high-amplitude, continuous reflections, and we interpret this seismic facies to be organic-rich lacustrine shale deposited mainly in a relatively deep lake, likely deeper than the modern basin, with only episodic desiccation or low lake conditions. Low lake conditions were likely to have occurred near the base-Kisegi boundary, where parasequences in Waki-B1 contain several thick sandstone units over a 150 m (492 ft) interval that stack in a progradational pattern, with minor aggradation (Figure 11). Deeper lake conditions are recorded in overlying parasequences, which display a clear transgressive systems tract with the development of thick, stacked beds of profundal sediments. Using the Waki-B1 well framework, we tentatively interpret the base-Kaiso surface to represent the Pliocene-Pleistocene boundary.

The seismic stratigraphic section above the base-Kaiso surface is markedly less continuous, with more variable seismic characteristics. We interpret the discontinuous reflections observed in the western, more deeply subsided, parts of the basin to be an indication of subaerial axial channelization over much of this interval. Such asymmetrical subsidence promotes avulsion of axial channels and focusing of the valley thalweg to the deeply subsided parts of the half-graben basin and is commonly observed in other rifts (Leeder and Gawthorpe, 1987; Scholz, 1995). The Waki-B1 lithology suggests that shallow lacustrine or deltaic environments may have prevailed in the eastern part of the basin. During this time, calcareous shale and clays, occasionally interbedded with thin ferruginous sandstones, dominate lithofacies in the well. Iron- and magnesium-rich sediments have been studied extensively in Lake Malawi (Williams and Owen, 1990; Owen et al., 1996) and have been observed forming in situ along the flexural margin of Lake Edward (Russell et al., 2003). The presence of ferruginous sandstones during this interval suggests exposure of previously buried sediments to oxic conditions at the sediment-water interface in a fluctuating depositional environment.

We correlate the mid-Kaiso surface to a thick sandstone interval documented in Waki-B1. The landscape in the rift valley at this time is interpreted as fluvial and channelized in the west and shallow lacustrine in the east. The climate system during this interval is increasingly arid, the lake experienced episodes of desiccation, and savannah landscapes may have periodically spread across the floor of the rift.

Above the mid-Kaiso surface in the northern part of the rift, we observe a distinct high-amplitude package of high-frequency and continuous reflections that is interpreted to be a section of fine-grained shale deposited under open lacustrine conditions. This seismic facies is especially prevalent in the center and eastern part of the Butiaba hanging wall (Figure 9). At the same stratigraphic interval in the far northwest of the basin, the very continuous reflection packages grade into less continuous facies and are interpreted to be evidence for increased amounts of coarser sediment and channeling during some intervals in this sequence. In the Waki-B1 well, parasequences are weakly aggradational to progradational near the mid-Kaiso surface, and profundal sediments are absent. We interpret this stacking pattern to reflect alluvial or lake-plain conditions along the eastern margin of the Butiaba footwall. Near 230 m (755 ft) depth in this well, organic-rich shale beds are again present in Waki-B1 and are juxtaposed with conglomerate beds. These stacking patterns appear to form sequence boundaries, but they do not correlate with any significant features in the seismic record. Therefore, we interpret this part of the vertical section to represent minor progradation during transgressive-regressive cycles in a shallow lake environment.

A basinwide unconformity in the shallow subsurface is widely observed in the MCS data set and likely developed in the late Quaternary (Karp et al., 2004). The most convincing evidence for this unconformity lies in prominent onlap and truncation reflection geometries, which are especially well expressed in the northern subbasin. For example, at the lake bottom on line 57, weak reflections onlap a high-amplitude continuous reflection from the west, suggesting rising water level following a low lake stand (Figures 4, 10). The depth of this unconformity varies with location in Lake Albert. In the northern subbasin, the unconformity surface is shallow in the east, especially on the Butiaba platform where recent sediment cover is less than 5 ms TWTT. The unconformity surface becomes buried in the west, however, where the maximum thickness of the late Quaternary sedimentary reaches approximately 40 ms

TWTT. This pattern of recent sedimentation is consistent with Lake Albert's structural architecture and suggests that after a recent period of reduced lake level, the deeply subsided part of the basin returned to open lake conditions before the sublittoral and uplifted platform regions in the northern subbasin. In the southern subbasin, this shallow unconformity is commonly between 10 and 20 ms TWTT below the modern lake bottom. The thick package of low-amplitude lens-shaped reflections overlying this unconformity surface is particularly intriguing. The bathymetric relief produced by this deposit created a zone of winnowing that has removed strata present in other areas of the basin. We interpret this unique sedimentary package to reflect increased discharge from the Nkusi and Semliki rivers following the most recent lowstand. Sediment core analysis conducted by Beuning et al. (1997) confirms the existence of a desiccation surface and pedogenic development in the lake during the late Quaternary.

We interpret the seismic stratigraphic framework identified in our data set to reflect the long-term changing environmental conditions in Africa since the mid-Miocene. Tectonic processes are factors in the development of the basin and in forcing adjustments to the upper Nile drainage network, of which Lake Albert is just a part. However, because of the overall simple structural framework of this basin and the apparent long-term and relatively consistent activity on the basin's main bounding faults, we interpret the primary changes in basin stratigraphy over time to be a consequence of short-term fluctuations in water balance in the system, overprinted on the well-documented long-term aridification of Africa since the late Miocene (deMenocal, 1995; Cane and Molnar, 2001). The considerable thickness of organic-rich shale at the base of the section is testimony to the prevalence of a relatively deep lake system for much of the late Miocene and Pliocene.

## SUMMARY AND CONCLUSIONS

1. Observations from seismic-reflection and gravity data sets reveal that the overall structural morphology of Lake Albert is that of a full graben, which is a unique configuration in the western rift valley. The Bunia border fault bounds the entire basin along the western shore, and it is opposed on the eastern margin by a complex of several large basement-involved faults, which created two structural subbasins. Major basement-involved faults control the modern distributions of isobaths and the location of deep-water areas. The maximum thickness of the sedimentary section is 5 km (3 mi) and dip on prerift basement is shallow (<1°).
2. The central (Tonya) region of the basin forms a large structurally complex relay ramp that may be a zone of major detrital sediment input. It may have been fed in the past by an ancient drainage that extended beyond the rift shoulder. Lake Albert's synrift sedimentary fill is best described as a thick sequence of relatively flat-lying sediments. Large-scale stratigraphic discordances are not present or are below the resolution of this seismic data set. Modern Lake Albert is overfilled and has alternated between a fluvial and lacustrine depositional system during the Quaternary. However, fine-grained organic-rich shales typify the lowermost sedimentary packages in the basin, indicative of fluctuating limnologic (balanced-filled) conditions during the basin's evolution.
3. A coarsening-upward pattern is observed in the stratigraphy of Lake Albert, and may be related to the overall aridification of Africa during the past approximately 7 m.y. This long-term aridification trend was punctuated early on by brief desiccation episodes and later by flooding events.
4. Evidence for prolonged desiccation events in the basin is present, defined by high-amplitude continuous reflections that can be traced basinwide. Evidence also exists for prolonged intervals of fluvial and alluvial deposition in the upper part of the section based on the character and geometry of seismic facies and by ties to Waki-B1 core stratigraphy.
5. The depositional history of this lake appears to have been conducive to the accumulation of the essential elements of an apparently significant petroleum system. Potential source rocks were deposited in overfilled deep lake conditions in the middle-upper Kisegi interval. Potential clastic reservoirs include sandstone and conglomerate intervals in the basal Kisegi, sandstone in the basal Kaiso, and sandstone and conglomerate in the upper Kaiso.

## ACKNOWLEDGMENTS

We thank the governments of Uganda and the Democratic Republic of the Congo for permission to conduct this research and to Hardman Resources Ltd. and partners for permission to study and present the seismic reflection data. This seismic reflection data set was acquired under extraordinarily difficult conditions, and we thank the Hardman Resources field team for their tireless efforts. We also thank members of the Syracuse University field team for their efforts: Jim McGill, Peter Cattaneo, Nick Peters, Phil Arnold, Kiram Lezzar, and Jannadi Lapunkeni. G. Karner generously

contributed bathymetric and gravity data that were incorporated into the analyses presented here. M. J. Soreghan and an anonymous reviewer provided helpful reviews.

## REFERENCES CITED

Abrahao, D., and J. E. Warme, 1990, Lacustrine and associated deposits in a rifted continental margin: Lower Cretaceous Lagoa Feia Formation, Campos Basin, offshore Brazil, *in* B. J. Katz, ed., Lacustrine basin exploration: Case studies and modern analogs: AAPG Memoir 50, p. 287–305.

Beadle, L. C., 1981, The inland waters of tropical Africa: An introduction to tropical limnology: London, Longman, 475 p.

Beuning, K. R. M., M. R. Talbot, and K. Kelts, 1997, A revised 30,000-yr paleoclimatic and paleohydrologic history of Lake Albert, East Africa: Paleogeography, Paleoclimatology and Paleoecology, v. 136, no. 1–4, p. 259–279, doi:10.1016/S0031-0182(97)00034-5.

Bishop, W. W., 1969, Pleistocene stratigraphy of Uganda: Geological Survey of Uganda Memoir X, 128 p.

Bohacs, K., A. Carroll, J. Neal, and P. Mankiewicz, 2000, Lake basin type, source potential, and hydrocarbon character: An integrated sequence-stratigraphic-geochemical framework, *in* E. Gierlowski-Kordesch and K. Kelts, eds., Lake basins through space and time: AAPG Studies in Geology 46, p. 3–34.

Bullard, E. C., 1936, Gravity measurements in East Africa: Philosophical Transactions of the Royal Society of London Series A, v. A235, p. 287–297.

Cane, M. A., and P. Molnar, 2001, Closing of the Indonesian seaway as a precursor to east African aridification around 3–4 million years ago: Nature, v. 411, p. 157–162, doi:10.1038/35075500.

Cassie, B., C. Sheen, and J. Wood, 2006, Exploration of the East African rift system in the Lake Albert area, Uganda: AAPG Search and Discovery article 90061, http://www.searchanddiscovery.net/abstracts/pdf/2006/intl_perth/abstracts/ndx_cassie.pdf (accessed April 2011).

Cohen, A., M. Soreghan, and C. Scholz, 1993, Estimating the age of formation of lakes: An example from Lake Tanganyika, East African rift system: Geology, v. 21, p. 511–514, doi:10.1130/0091-7613(1993)021<0511:ETAOFO>2.3.CO;2.

Demaison, G. J., and G. T. Moore, 1980, Anoxic environments and oil source bed genesis: AAPG Bulletin, v. 64, no. 8, p. 1179–1209.

deMenocal, P. B., 1995, Plio–Pleistocene African climate: Science, v. 270, no. 5233, p. 53–59, doi:10.1126/science.270.5233.53.

Ebinger, C. J., 1989, Tectonic development of the western branch of the East African rift system: Geological Society of America Bulletin, v. 101, p. 952–967, doi:10.1130/0016-7606(1989)101<0952:TAEOAM>2.3.CO;2.

Ebinger, C. J., A. L. Deino, A. L. Tesha, T. Becker, and U. Ring, 1993, Tectonic controls on rift basin morphology: Evolution of the northern Malawi (Nyasa) rift: Journal of Geophysical Research, v. 98, no. B10, p. 17,821–17,836.

Frostick, L., and I. Reid, 1989, Is structure the main control on river drainage and sedimentation in rifts?: Journal of African Earth Sciences, v. 8, p. 165–182, doi:10.1016/S0899-5362(89)80022-3.

Gawthorpe, R. L., and M. R. Leeder, 2000, Tectono-sedimentary evolution of active extensional basins: Basin Research, v. 12, p. 195–218, doi:10.1046/j.1365-2117.2000.00121.x.

Götze, H.-J., 1978, Ein numerisches Verfahren zur Berechnung der gravimetrischen Feldgrößen drei-dimensionaler Modellkörper: Archiv für Meterologie, Geophysik und Bioklimatologie. Serie A, Meteorologie und Geophysik, v. 25, p. 195–215.

Götze, H.-J., and B. Lahmeyer, 1988, Application of three-dimensional interactive modeling in gravity and magnetics: Geophysics, v. 53, no. 8, p. 1096–1108, doi:10.1190/1.1442546.

Harris, N., J. W. Pallister, and J. M. Brown, 1956, Oil in Uganda: Memoir IX, Geological Survey and Mines Department, Entebbe, Uganda, 33 p.

Johnson, T. C., E. T. Brown, J. McManus, S. Barry, P. Barker, and F. Gasse, 2002, A high-resolution paleoclimate record spanning the past 25,000 years in southern East Africa: Science, v. 295, p. 113–114, 131–132, doi:10.1126/science.1070057.

Karner, G. D., B. R. Byamungu, C. J. Ebinger, A. B. Kampunzu, R. K. Mukasa, J. Nyakaana, E. N. T. Rubondo, and N. M. Upcott, 2000, Distribution of crustal extension and regional basin architecture of the Albertine Rift System, East Africa: Marine and Petroleum Geology, v. 17, p. 1131–1150, doi:10.1016/S0264-8172(00)00058-1.

Karp, T., M. M. McGlue, C. A. Scholz, F. Kasande, and F. Mugisha, 2004, Extensional tectonics and paleoclimate of the Albertine and Edward rifts: Constraints from integrated seismic reflection and topographic studies (abs.): Eos Transactions, American Geophysical Union, 85(47), Fall Meeting Abstract U21A-0702.

Katz, B. J., 1990, Controls on distribution of lacustrine source rocks through time and space, *in* B. J. Katz, ed., Lacustrine basin exploration: Case studies and modern analogs: AAPG Memoir 50, p. 61–76.

Lambiase, J. J., 1990, A model for tectonic control of lacustrine sequences in continental rift basins, *in* B. Katz, ed., Lacustrine basin exploration: Case studies and modern analogs: AAPG Memoir 50, p. 265–274.

Leeder, M. R., and R. L. Gawthorpe, 1987, Sedimentary models for extensional tilt-block/half-graben basins, *in* M. P. Coward, J. F. Dewey, and P. L. Hancock, eds., Continental extensional tectonics: Geological Society (London) Special Publication 28, p. 139–152.

McHargue, T. R., 1990, Stratigraphic development of proto-South Atlantic rifting in Cabinda, Angola: A petroliferous

lake basin, *in* B. J. Katz, ed., Lacustrine basin exploration: Case studies and modern analogs: AAPG Memoir 50, p. 307–326.

Modisi, M. P., E. A. Atekwana, A. B. Kampunzu, and T. H. Ngwisanyi, 2000, Rift kinematics during the incipient stages of continental extension: Evidence from the nascent Okavango Rift Basin, Northwest Botswana: Geology, v. 28, p. 939–942, doi:10.1130/0091-7613(2000)28<939:RKDTIS>2.0.CO;2.

Morley, C. K., 1988, Variable extension in Lake Tanganyika: Tectonics, v. 7, p. 785–801, doi:10.1029/TC007i004p00785.

Morley, C. K., 1989, Extension, detachments and sedimentation in continental rifts (with particular reference to East Africa): Tectonics, v. 8, p. 1175–1192, doi:10.1029/TC008i006p01175.

Nelson, R. A., T. L. Patton, and C. K. Morley, 1992, Rift segment interaction and its relation to hydrocarbon exploration in continental rift systems: AAPG Bulletin, v. 76, p. 1153–1169.

Nyblade, A. A., and R. A. Brazier, 2002, Precambrian lithospheric controls on the development of the East African rift system: Geology, v. 30, p. 755–758, doi:10.1130/0091-7613(2002)030<0755:PLCOTD>2.0.CO;2.

Nyblade, A. A., and C. A. Langston, 1995, East African earthquakes below 20 km depth and their implications for crustal structure: Geophysical Journal International, v. 121, p. 49–62, doi:10.1111/j.1365-246X.1995.tb03510.x.

Owen, R. B., R. W. Renaut, and T. W. Williams, 1996, Characteristics and origins of laminated ferromanganese nodules from Lake Malawi, Central Africa, *in* T. C. Johnson and E. O. Odada, eds., The limnology, climatology and paleoclimatology of the East African lakes: Amsterdam, The Netherlands, Gordon and Breach, p. 461–474.

Reynolds, D. J., and B. R. Rosendahl, 1984, Tectonic expressions of continental rifting: EOS Transactions of the American Geophysical Union, v. 65, no. 45, p. 1116.

Ring, U., C. Betzler, and D. Delvaux, 1992, Normal vs. strike-slip faulting during rift development in East Africa; the Malawi Rift: Geology, v. 20, no. 11, p. 1015–1018, doi:10.1130/0091-7613(1992)020<1015:NVSSFD>2.3.CO;2.

Rosendahl, B. R., 1987, Architecture of continental rifts with special reference to East Africa: Annual Review of Earth and Planetary Science, v. 15, p. 445–503.

Rosendahl, B. R., D. J. Reynolds, P. M. Lorber, C. F. Burgess, J. McGill, D. Scott, J. J. Lambiase, and S. J. Derksen, 1986, Structural expressions of rifting: Lessons from Lake Tanganyika, *in* L. E. Frostick, R. W. Renaut, I. Reid, and J. J. Tiercelin, eds., Sedimentation in the African rifts: Geological Society (London) Special Publication 25, p. 29–44.

Rosendahl, B. R., J. Versfelt, C. A. Scholz, and L. D. Woods, 1988, Seismic atlas of Lake Tanganyika, East Africa: Project PROBE: Durham, North Carolina, Duke University, 82 p.

Russell, J. M., T. C. Johnson, K. Kelts, T. Laerdal, and M. R. Talbot, 2003, An 11,000-year lithostratigraphic and paleohydrologic record from equatorial Africa: Lake Edward, Uganda-Congo: Palaeogeography, Palaeoclimatology and Palaeoecology, v. 193, p. 25–49, doi:10.1016/S0031-0182(02)00709-5.

Scholz, C. A., 1995, Deltas of the Lake Malawi rift, East Africa: Seismic expression and exploration implications: AAPG Bulletin, v. 79, no. 11, p. 1679–1697.

Scholz, C. A., 2001, Applications of seismic sequence stratigraphy in lacustrine basins, *in* W. M. Last and J. P. Smol, eds., Tracking environmental changes in lake sediments: Physical and chemical techniques: Dordrecht, Netherlands, Kluwer Academic Publishers, p. 7–22.

Scholz, C. A., B. R. Rosendahl, J. W. Versfelt, K. J. Kaczmarick, and L. D. Woods, 1989, Seismic atlas of Lake Malawi (Nyasa), East Africa: Project PROBE: Durham, North Carolina, Duke University, 116 p.

Scholz, C. A., B. R. Rosendahl, and D. L. Scott, 1990, Development of coarse-grained facies in lacustrine rift systems: Examples from East Africa: Geology, v. 18, p. 140–144, doi:10.1130/0091-7613(1990)018<0140:DOCGFI>2.3.CO;2.

Scholz, C. A., T. C. Johnson, and J. W. McGill, 1993, Deltaic sedimentation in a Rift Valley Lake: New seismic reflection data from Lake Malawi (Nyasa), East Africa: Geology, v. 21, p. 395–398, doi:10.1130/0091-7613(1993)021<0395:DSIARV>2.3.CO;2.

Scholz, C. A., J. W. King, G. S. Ellis, P. K. Swart, J. C. Stager, and S. M. Colman, 2003, Paleolimnology of Lake Tanganyika, East Africa, over the past 100 k yr: Journal of Paleolimnology, v. 30, p. 139–150, doi:10.1023/A:1025522116249.

Smith, B., and J. Rose, 2002a, Uganda's Albert Graben due to first serious exploration test: Oil & Gas Journal, v. 100, no. 23, p. 42–48.

Smith, B., and J. Rose, 2002b, Meeting exploration challenges in Uganda's remote Albert Graben: Oil & Gas Journal, v. 100, no. 24, p. 36–39.

Soreghan, M. J., and A. S. Cohen, 1996, Textural and compositional variability across littoral segments of Lake Tanganyika: The effect of asymmetric basin structure on sedimentation in large rift lakes: AAPG Bulletin, v. 80, p. 382–409.

Soreghan, M. J., C. A. Scholz, and T. J. Wells, 1999, Coarse-grained deep-water sedimentation along a border fault margin of Lake Malawi, Africa: Journal of Sedimentary Research, v. 69, p. 832–846.

Strecker, M. R., P. M. Blisniuk, and G. H. Eisbacher, 1990, Rotation of extension direction in the Central Kenya rift: Geology, v. 18, no. 4, p. 299–302, doi:10.1130/0091-7613(1990)018<0299:ROEDIT>2.3.CO;2.

Talbot, M. R., 1988, The origins of lacustrine oil source rocks: evidence from the lakes of tropical Africa, *in* A. J. Fleet, K. Kelts, and M. R. Talbot, eds., Lacustrine petroleum source rocks: Geological Society (London) Special Publication 40, p. 29–43.

Tiercelin, J.-J., A. S. Cohen, M. J. Soreghan, and K. E. Lezzar, 1992, Pleistocene-modern deposits of the Lake Tanganyika Rift Basin, East Africa: A modern analog for lacustrine source rocks and reservoirs, *in* A. J. Lomando, C. Schreiber, and P. M. Harris, eds., Lacustrine reservoirs and depositional systems: SEPM Core Workshop 19, p. 37–59.

Upcott, N. M., R. Mukasa, and C. J. Ebinger, 1996, Along-axis segmentation and isostasy in the western rift, East Africa: Journal of Geophysical Research, v. 101, p. 3247–3268, doi:10.1029/95JB01480.

Van Wagoner, J. C., R. M. Mitchum, K. M. Campion, and V. D. Rahmanian, 1990, Siliciclastic sequence stratigraphy in well logs, cores, and outcrops: AAPG Methods in Exploration Series 7, 55 p.

Versfelt, J., and B. R. Rosendahl, 1989, Relationship between pre-rift structure and rift architecture in lakes Tanganyika and Malawi, East Africa: Nature, v. 337, p. 3–356.

Williams, T. M., and R. B. Owen, 1990, Authigenesis of ferric oolites in superficial sediments from Lake Malawi, Central Africa: Chemical Geology, v. 89, p. 179–188, doi:10.1016/0009-2541(90)90066-G.